Journal of Advanced Research (2016) 7, 863–871

Cairo University

Journal of Advanced Research

ORIGINAL ARTICLE

Mechanochemical synthesis of chitosan submicron particles from the gladius of *Todarodes pacificus*

J.R. Anusha [a], Albin T. Fleming [a], M. Valan Arasu [b], Byung Chul Kim [c], Naif Abdullah Al-Dhabi [b], Kook-Hyun Yu [c], C. Justin Raj [c,*]

[a] *Department of Advanced Zoology and Biotechnology, Loyola College, Chennai 600034, India*
[b] *Department of Botany and Microbiology, Addiriyah Chair for Environmental Studies, College of Science, King Saud University, P.O. Box 2455, Riyadh 11451, Saudi Arabia*
[c] *Department of Chemistry, Dongguk University-Seoul, Seoul 100715, Republic of Korea*

GRAPHICAL ABSTRACT

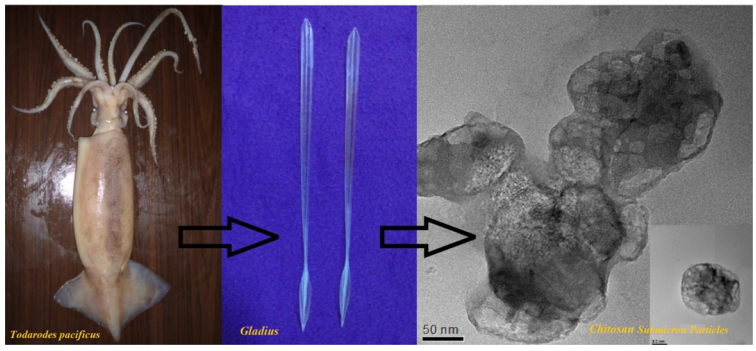

Scheme for the synthesis of chitosan submicron particles from gladius of squid, *Todarodes pacificus*.

ARTICLE INFO

Article history:
Received 16 June 2016
Received in revised form 23 August 2016

ABSTRACT

The present work focused on the synthesis of β-chitosan submicron particles (CSPs) from *Todarodes pacificus* using mechanochemical techniques. The gladius was submitted to a sequence of mechanical and chemical treatments to synthesize β-chitin (CT), which was further deacetylated to form spherical chitosan submicron particles with an average diameter of

* Corresponding author.
E-mail address: cjustinraj@gmail.com (C. Justin Raj).
Peer review under responsibility of Cairo University.

Production and hosting by Elsevier

http://dx.doi.org/10.1016/j.jare.2016.08.006

Accepted 25 August 2016
Available online 4 September 2016

Keywords:
Gladius
β-chitin
Chitosan
Submicron particles
Mechanochemical synthesis

⩽100 nm. The surface morphology of β-chitin and CSPs was observed using electron microscopy. The degree of deacetylation (DD%), evaluated from the absorbance peak of a Fourier Transform Infrared (FTIR) spectrum, was 80 ± 2.5%. Physicochemical characterization exhibited good crystallinity, positive zeta potential and low molecular weight, as well as reduced ash content and high water-binding capacity. CSPs exhibit significant antimicrobial properties toward all tested pathogenic bacterial and fungal microorganisms. Antioxidant analysis revealed high reducing power and excellent scavenging and chelating ability. Hence, CSPs synthesized from gladius of *Todarodes pacificus* using mechanochemical techniques are promising candidates for biomedical applications.

Introduction

Chitosan (CS) is a functional biopolymer and linear polysaccharide obtained from chitin (CT) that has attracted significant interest in biomedical, food, textile and chemical industries. Chitin is a naturally abundant mucopolysaccharide found in wide range of natural sources such as crustaceans, insects, annelids, molluscs, coelenterates, and zygomycetes fungi [1–3]. Depending on the source, CT exists in three different polymorphic forms: α-, β- and γ-chitin, which differ in the arrangement of chains within the crystalline region, leading to distinct networks of hydrogen bonds [4]. Chitin is a hard, inelastic material that is insoluble in most solvents due to its compact structure. The deacetylated derivative chitosan possesses excellent biodegradability, biocompatibility, non-toxicity and bioactivity and is therefore well positioned for a wide range of industrial and medical applications [5].

Commercial CS is produced using CT from shrimp and crab shells as raw materials, requiring high production costs and multiple chemical processing steps including demineralization, deproteinization and decolorization. Another rich source of CT is squid gladius, which is a transparent material discarded as waste by the seafood processing industry [6]. The CS extraction procedure from squid gladius requires minimal quantities of acid and alkaline chemicals due to an absence of colored compounds and fewer impurities, which reduces production costs and environmental pollution [7]. Due to its weaker intermolecular hydrogen bonds, solubility, quality and swelling compared to α-CT, chitosan produced from gladius has good physicochemical and functional properties when compared with other crustacean sources.

Recently, CS and its derivative based soluble and particulate carriers have attracted unique interest from the biomedical field. Drugs can be encapsulated in a CS matrix to improve their therapeutic efficiency and bioavailability. The mucoadhesive property of CS facilitates the administration of poorly absorbable drugs and macromolecules such as DNA, siRNA, growth factors, and antigens across epithelial barriers [8,9]. Chitosan has been used in tissue engineering for skin repair and wound healing using regeneration mechanisms [10]. It also has biological activities, including antimicrobial [11], antioxidant [12], antitumor [13], anti-inflammatory [14], immune stimulatory [15], and anti-hepatotoxicity [16] properties.

Generally, CS with unique nano or submicron structures can be fabricated using coagulation or precipitation, covalent crosslinking, ionic crosslinking, emulsion droplet coalescence methods [17] or ionic gelation processes with sodium tripolyphosphate and the addition of polyanions [18]. Very few attempts have been made to synthesize submicron or nanosized CS particles from the gladius of squid with minimal chemical treatment. Therefore, the major objective of this study was to fabricate CSPs from *Todarodes pacificus* squid gladius using simple mechanochemical techniques. The CSPs prepared by this process were subjected to various physicochemical analyses including Fourier-Transform Infrared (FT-IR) spectroscopy, X-Ray Diffraction (XRD), scanning electron microscopy (SEM) and transmission electron microscopy (TEM). CSPs were also tested for antimicrobial and antioxidant properties. The aim of this study was to contribute a method for generating CS particles from a renewable gladius resource with less chemical treatment for future applications.

Material and methods

Materials

Commercially available chitosan from crab (Std. CS) [Low MW ~ 150 kDa, DD-75 to 85%] was purchased from Sigma-Aldrich, Seoul, Republic of Korea. Sodium hydroxide, hydrochloric acid, and ethanol were purchased from Daejung Chemicals, Seoul, Republic of Korea. The media and reagents for antimicrobial and antioxidant studies were purchased from Hi-Media, Mumbai, India. All chemicals were of reagent grade and used without further purification. The gladius of squid (*Todarodes pacificus)* was collected from Jagalchi fish market, Busan, Republic of Korea. The gladius (length ~18.5 cm, width ~1.3 cm and thickness ~0.54 mm) was separated from the squid and then washed, cleaned, dried at 30 °C, and stored in refrigerator (4 °C) for analysis.

β-Chitin extraction from gladius

Dried gladius was cut into small pieces and ground using a ball mill (Retsch, Model PM-100) for 1 h at 600 rpm to form a fine powder. From the powdered gladius, CT was extracted using a sequence of processes including deproteinization using 1 M NaOH at 50 °C for 5 h and demineralization in 1 M HCl at room temperature for 2 h under constant stirring.

Mechanochemical synthesis of CSPs

The CT powder prepared from gladius was added to 50% NaOH with a solid-to-alkaline solution ratio of 1:15 (w/v) at 60 ± 5 °C under nitrogen atmosphere for 2 h with constant stirring. The treatment was repeated thrice, each time with freshly prepared NaOH solution. The pure white suspension produced was centrifuged, filtered, and dried at room temper-

ature. The dried CS powder was pulverized and converted to an ultra-fine powder by a ball-milling process (Retsch, Model PM-100).

Physicochemical characterization

The morphologies of CT and CSPs were recorded using transmission and scanning electron microscopy. SEM images of the samples were collected. XRD patterns of CT and CSPs were obtained using an X-ray diffractometer (D/MAX-2200, Rigaku Co., Japan) with Cu Kα radiation with a wavelength of 0.154 nm. The scattering intensities were measured over an angle range of 10–80° (2θ) with a scanning rate of 2°/min. The relative crystallinity index (*CI*) of CT and CSPs was calculated using the following equation [19]:

$$Crystallinity\ Index\ (CI\ \%) = (I_{110} - I_{am})/I_{110} \times 100 \quad (1)$$

where I_{110} (arbitrary units) is the maximum intensity of the (1 1 0) peak, which is usually approximately $2\theta = 20°$, and I_{am} (arbitrary units), which is the amorphous diffraction at $2\theta = 16°$.

$$D_{app}(110) = k\lambda/\beta(cos(\theta)) \quad (2)$$

Degree of deacetylation

The degree of deacetylation (DD) was evaluated from the FTIR absorbance peak at 1655 cm^{-1} for amide-I, and at 3450 cm^{-1} for the OH of CSPs according to the method of Baxter et al. [20], as shown in the following equation:

$$DD = [(A_{1655}/A_{3450}) \times 115] \quad (3)$$

where A_{1655} and A_{3450} are the absorbance at 1655 cm^{-1} and 3450 cm^{-1}, respectively.

Analysis of chemical properties

The average molecular weight (M_v) was measured using a viscoscopic method [21]. M_v was calculated using the Mark-Houwink equation:

$$[\eta] = K(M_v)^{\alpha} \quad (4)$$

where [η] and M_v represent intrinsic viscosity and viscosity molecular weight, and K and α are viscometric constants with literature values of 1.81×10^{-5} and 0.93, respectively.

The Zeta potential of CSPs was analyzed using a Zeta sizer (Malvern Instruments, Malvern, UK) using a dynamic light scattering method. The ash and moisture contents were estimated as described in AOAC [22] and Wang and Kinsella [23]. For the analysis of WBC and FBC, 0.5 g of sample was kept in a 50-mL centrifuge tube, and 10 mL of water or soybean oil was added and mixed thoroughly for 1 min on a vortex mixer.

Antimicrobial activity

Antimicrobial activity assays were performed for CT, CSPs and Std. CS samples using a Kirby-Bauer disk diffusion method with slight modifications [24]. For antibacterial assays, both gram-positive and gram-negative bacteria were lawn-cultured on nutrient agar plates with sample-loaded disks and incubated at 37 °C for 24 h. Bacterial strains such as *Lactobacillus brevis, Micrococcus* sp., *Staphylococcus aureus, Streptococcus* sp., *Aeromonas hydrophila, Enterobacter* sp., *Escherichia coli*, and *Proteus vulgaris* were used in these antimicrobial assays. To perform the *in vitro* antifungal assay, the surface of sabouraud dextrose agar (SDA) plates was seeded with 0.1 mL of a spore suspension (10^4 spores/mL). Disks loaded with samples were placed on SDA plates and incubated at 25 °C for 3–5 days. To calculate disk diffusion, the zone of growth inhibition was measured and analyzed. The standard antibiotic ofloxacin served as a positive control and filter disks impregnated with 10 µL solvent (distilled water and DMSO) were used as a negative control.

Determination of antioxidant

Reducing power assay

Reducing power was determined by assessing the ability of CSPs to reduce a $FeCl_3$ solution, as described by Yen et al. [25].

Superoxide radical scavenging assay

The superoxide radical scavenging ability of CSPs was assessed using the method of Jing [26]. Various concentrations of samples (1.0–5.0 mg/mL) were added to 100 µL of riboflavin solution (20 µg), 200 µL of EDTA solution (12 mM), 200 µL of methanol and 100 µL of nitro-blue tetrazolium (NBT) solution (0.1 mg). The percent scavenging activity was calculated using Eq. (5):

$$Scavenging\ activity\ (\%) = \frac{1 - Absorbance\ (test)}{Absorbance\ (blank)} \times 100 \quad (5)$$

Scavenging ability on 1,1-diphenyl-2-picrylhydrazyl (DPPH) radicals

The scavenging ability of DPPH radicals was determined following the method of Ramasamy et al. [27]. The scavenging ability of CSPs was calculated using the following formula:

$$Scavenging\ ability = \frac{Absorbance\ of\ control - Absorbance\ of\ test}{Absorbance\ of\ control} \times 100 \quad (6)$$

Chelating ability to ferrous ions

The chelating ability of CSPs to ferrous ions was determined with respect to ethylenediaminetetraacetic acid (EDTA) [28].

Statistical analysis

Each experiment was performed in triplicate and the results shown are mean values ± standard deviation (SD). For data analysis, Origin Pro 8 (Origin Lab Corporation) was used.

Results and discussion

Extraction of β-CT and CSPs

Because of the higher purity of the endoskeleton gladius raw material, fewer steps were needed to demineralize and deproteinize during the synthesis of β-CT. The average weight of each dried gladius was 0.345 ± 0.082 g, which was calcu-

lated based on 50 intact gladii. Approximately 0.078 g of water-insoluble white fibrous β-CT was obtained from each gladius, with a total yield of ~42–43%, in agreement with previous reports [29].

Morphological studies of CT and CSPs

Fig. 1a and b shows SEM images of ball-milled CTs for two different magnifications. It is clear that the samples show nanofiber morphology with widths from 50 nm to 500 nm and lengths greater than 10 micrometers. The SEM reveals that the ball-milling of CT reduces the size of samples. SEM images of the final CSPs are shown in Fig. 1c and d. The sample displays agglomeration of submicron particles with irregular morphology, as observed in most polymeric samples. For further understanding of the morphology, the samples were subjected to TEM analysis.

The close-up views of TEM images of CT show that the sample is composed of needle-shaped crystallites of β-CT (Fig. 2a and b). Moreover, it confirms that mechanochemically synthesized CS samples are composed of large numbers of spherical submicron particles in an agglomerated form (Fig. 2c and d) [17]. From Fig. 2d, one can easily observe very small crystallites of less than 1 nm on the surface of spherical CSPs.

FT-IR spectrophotometer

The FTIR spectra of CT and CSPs are shown in Fig. 3a. A single band was observed at 1666 cm^{-1} for CT and 1671 cm^{-1} for CSPs, indicating that the amide groups form hydrogen bonds [19]. Various vibrational modes for CH_2 bending and CH_3 deformation were found at 1558 and 1378 cm^{-1} for CT. A well-defined band at 1467 cm^{-1} denotes the amide I band of CT. The two major peaks at 1671 cm^{-1} and 1564 cm^{-1} were assigned to the C═O stretching (amide I) and NH bending vibration (amide II), respectively. For CSPs, a specific band appeared at 1322 cm^{-1}, which confirmed the presence of N-acetyl-glucosamine. An asymmetrical bridge with oxygen stretching and asymmetrical in-phase ring stretching vibrational modes were observed for CT (1157 and 1114 cm^{-1}) and CSPs (1159 cm^{-1}), respectively. The peak is approximately 1655 cm^{-1} with C═O stretching for the secondary amide and its intensity depended on the extent of the deacetylation of the sample.

The DD%, calculated using FTIR spectra, was 80 ± 2.5% for CSPs synthesized from *T. pacificus*. DD increases with increasing NaOH concentration and deacetylation time [30].

X-ray diffraction analysis

X-ray diffraction was used to detect the crystallinity and crystallite size of CT and CSPs. XRD patterns for CT and CSPs are shown in Fig. 3(b). Both spectra show a broad diffraction peak at 20–23°, which was assigned as the prominent diffraction peak of (1 1 0) for CT and CSPs samples. This peak characterizes the hydrated crystal line structure of CT and ensures the presence of crystalline CSPs. The peak intensity of CSPs was found to be higher than for CT, representing higher CSPs crystallinity in agreement with the previous report by Muzzarelli et al. [31], where the crystallinity index of CT was

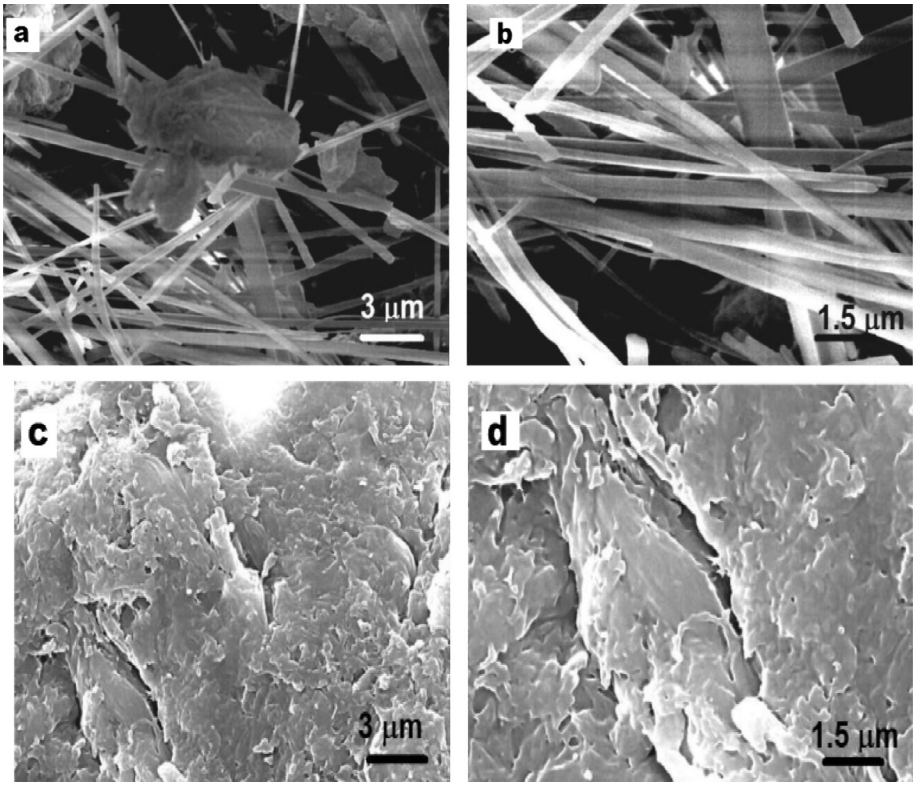

Fig. 1 SEM images of CT (a, b) and CSPs (c, d) at two different magnifications.

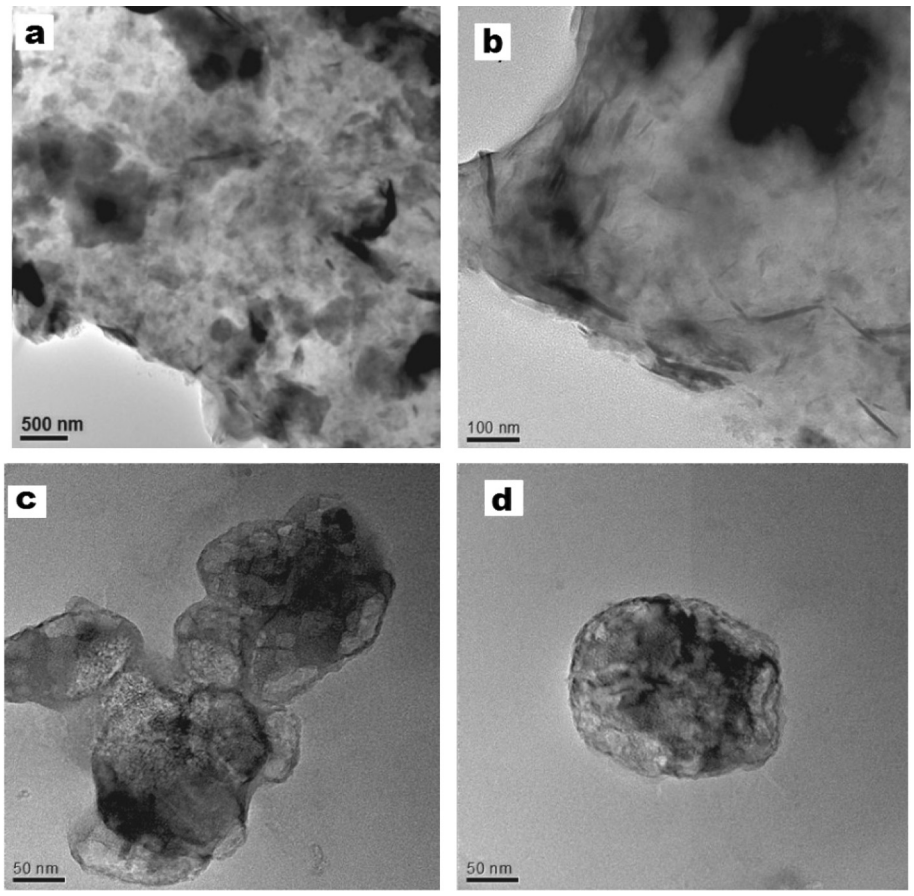

Fig. 2 TEM images of CT (a and b) showing nanofiber morphology and image of CSPs (c and d) depicting spherical submicron particles.

24.6%, and CSPs showed a superior crystallinity of 45.5%. The apparent crystallite size of CSPs was calculated to be ~0.41 nm, in agreement with crystallites observed in the TEM images of CS spherical submicron particle surfaces.

Chemical properties of CSPs

The molecular weight determined using viscometry was 118.54 kDa for CSPs. The molecular weight of CS from gladius was found to be less than that of commercial chitosan obtained from crab, prawn, molluscs and shrimp [32]. The variation in molecular weight may be due to the source of CS and may vary with parameters such as intermolecular hydrogen bonding, dissolved oxygen concentration, chitin concentration, particle size, reaction time, and concentration of alkali (Fig. 4).

General studies were carried out to analyze the chemical properties of CSPs from gladius of the squid *T. pacificus*. The ash content and moisture content for CSPs were 0.12 ± 0.20% and 2.04 ± 0.15%, respectively. Due to this very low ash content, overall production costs may be reduced and less acid needed for processing [3]. The water-binding capacities of CT and CSPs were 6.28 ± 0.1X% and 5.42 ± 0.2X%, whereas the fat binding capacities were 1.89 ± 0.12X% and 1.86 ± 0.12X%, respectively. Both CSPs and CT showed high water absorbance, consistent with their highly hygroscopic nature. These CSP results are comparable to the reports by Reys et al. [5] and Youn et al. [6].

Antimicrobial activity

The antimicrobial activity of CT and CS derivatives has been recognized as the most important property for biomedical applications. For antimicrobial activity, CT, CSPs and Std. CS were tested against various pathogenic microorganisms, and the results are listed in Table 1. The highest inhibition zone by CSPs was found for the Gram-negative bacteria *Escherichia coli* (24 ± 0.35 mm) followed by the Gram-positive bacteria *Micrococcus* sp. (22 ± 0.5 mm). In the case of fungal organisms, CSPs showed high activity for *Rhizopus* sp., with a 23 ± 0.5 mm, zone of inhibition. Chitin and Std. CS showed large zones of inhibition and significant activity against *E. coli*. Among other bacterial species, *Staphylococcus aureus* showed a reasonable rate of activity in all the samples, followed by *Streptococcus* sp., *Enterobacter* sp., *Lactobacillus*, and *Proteus vulgaris*. For fungal species, *Aspergillus niger* and *A. flavus* showed moderate levels of inhibition for CSPs. Among the tested microbes, all three samples failed to show activity for *Penicillium* sp. The best antimicrobial properties were displayed by CSPs followed by Std. CS and CT.

The antimicrobial activity of CSPs may be due to electrostatic forces between positively charged CSPs and negatively

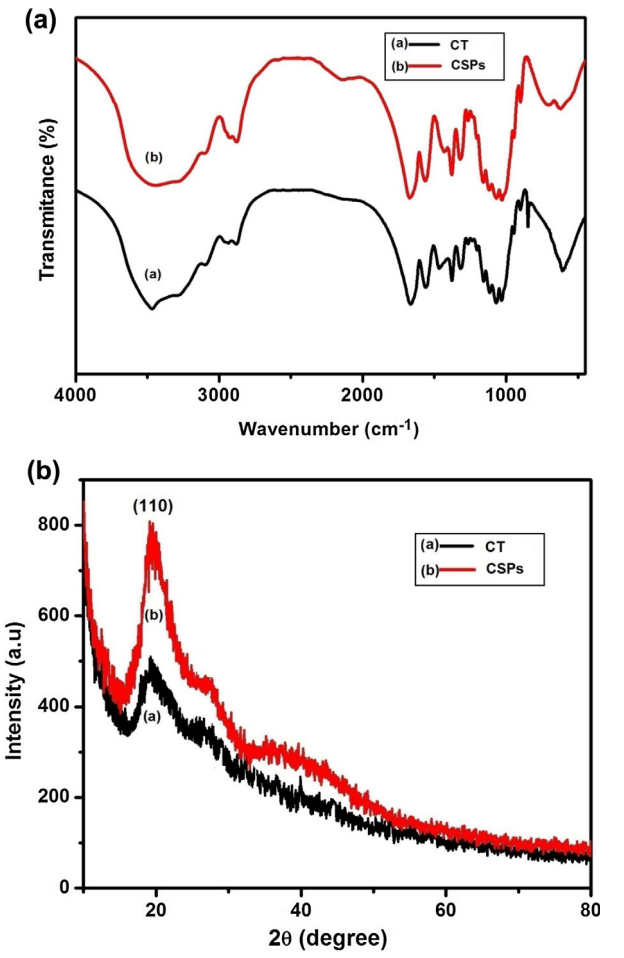

Fig. 3 (a) Fourier-Transform Infrared spectra (FTIR) and (b) X-ray diffraction pattern of CT and CSPs.

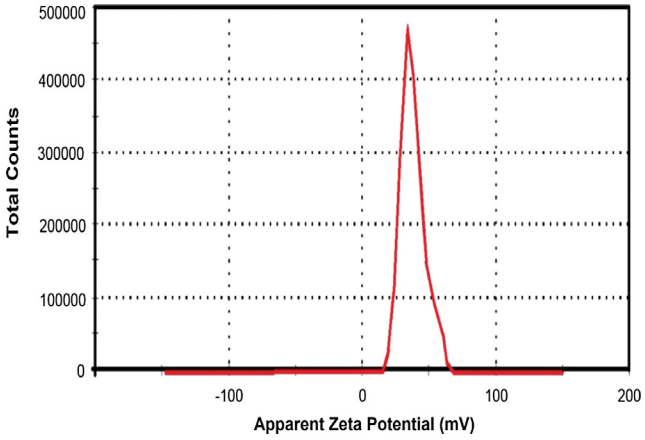

Fig. 4 Zeta potential of CSPs synthesized from the gladius of the squid *T. pacificus*.

charged microbial cell walls that interrupt the normal cell mechanism related to bacterial DNA, thus inhibiting RNA synthesis [33]. CSPs may enter into the cell and bond more easily than normal-sized Std. CS [11].

Antioxidant potential analysis

Reducing property

The reducing ability of CSPs extracted from the gladius of *T. pacificus* using mechanochemical methods was investigated. At a concentration of 2 mg/mL, the CSPs showed a lower reducing power of 0.65 Abs, while at higher concentration (10 mg/mL), the reducing power was 1.32 Abs. The reducing power of CSP samples correlates very well with increasing concentration (Fig. 5); values remained lower than those of ascorbic acid (1.65 Abs.) and higher than those of the Std. CS (1.15 Abs.) at 10 mg/mL concentration. Yen et al. reported low reducing power (0.13–0.29 Abs.) at 1 mg/mL for fungally extracted CS from shiitake stipes and a moderate reducing power (0.42–0.57 Abs.) [34]. In addition, Yen et al. tested crab CS and reported a reducing power of 0.32–0.44 Abs. at 10 mg/mL [25].

Superoxide radical scavenging ability

The superoxide radical scavenging ability of CSPs is concentration-dependent, in the range of 25.2–61.7% for concentrations of 0.1–0.5 mg/mL (Fig. 6). The IC_{50} value calculated for CSPs was 0.369. The ascorbic acid control exhibited high scavenging capacities of 65.30% at 0.5 mg/mL. The scavenging activity for Std. CS against superoxide was 46.12% at 0.5 mg/mL, with IC_{50} values of 0.49. The IC_{50} reported against superoxide radicals for CS from *P. vigil* at 0.5 mg/mL was at 31.47% [35], comparatively lower than that in the present investigation.

Scavenging ability on 1,1-diphenyl-2-picrylhydrazyl (DPPH) radicals

The scavenging ability of CSPs on DPPH radicals was found to be 76.38% at 10 mg/mL (Fig. 7). At 10 mg/mL, the ascorbic acid used as a standard showed higher scavenging abilities of 79.9%. Thus, CSPs from squid gladius are moderately active against DPPH radicals. The IC_{50} of CSPs was 0.47 mg/mL, which is significant compared to previous reports [27].

Chelating ability on ferrous ions

The ferrous-ion chelating effect of CSPs was concentration-dependent. At different concentrations (0.1–10 mg/mL), CSPs values ranged from 44.3% to 74.1% (Fig. 8), higher than those for Std. CS (40.6–64.8%). The IC_{50} values were 0.59 mg/mL and 1.06 mg/mL for CSPs and Std. CS, respectively. The EDTA control showed the highest chelating ability of 79.8% at 10 mg/mL with an IC_{50} value of 0.11 Abs. In previous studies, the chelating ability of CS from *P. vigil* with ferrous ion ranged from 25.82% to 73.54% when concentration varied from 0.1 to 10 mg/mL [35–38].

Conclusions

Chitosan submicron-sized particles were successfully synthesized by mechanochemical means from β-CT extracted from the gladius of *T. pacificus*. Physiochemical studies revealed an excellent degree of deacetylation, crystallinity, morphology and low molecular weight along with very low ash content and high water-binding capacity. These materials exhibit better antimicrobial activity than commercially available Std. CS, mainly due to their submicron size and positive charge.

Table 1 Antimicrobial activity of chitin, chitosan submicron particles and standard chitosan.

Microorganism	Chitin (CT)	Chitosan submicron particles (CSPs)	Standard Chitosan (Std. CS)
	Zone of inhibition (mm)		
Lactobacillus brevis	NZ	10 ± 0.5	7 ± 0.5
Micrococcus sp.	10 ± 0.125	22 ± 0.5	19 ± 0.25
Staphylococcus aureus	12 ± 0.25	20 ± 0.125	16 ± 0.25
Streptococcus sp.	6 ± 0.15	9 ± 0.5	NZ
Aeromonas hydrophila	NZ	10 ± 0.15	NZ
Enterobacter sp.	8 ± 0.25	11 ± 0.25	NZ
Escherichia coli	18 ± 0.5	24 ± 0.35	20 ± 0.25
Proteus vulgaris	NZ	11 ± 0.15	8 ± 0.3
Aspergillus flavus	9 ± 0.7	12 ± 0.5	NZ
Aspergillus niger	NZ	21 ± 0.2	20 ± 0.3
Rhizopus sp.	10 ± 0.25	23 ± 0.5	19 ± 0.15
Candida sp.	9 ± 0.6	17 ± 0.4	NZ
Penicillium sp.	NZ	NZ	NZ

NZ: No Zone of Inhibition; Values were the means ± standard deviation of 3 replications ($n = 3$).

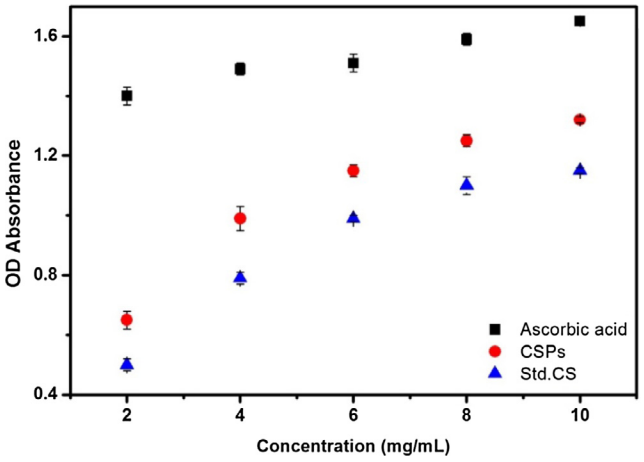

Fig. 5 Reducing power of ascorbic acid, CSPs, and Std. CS.

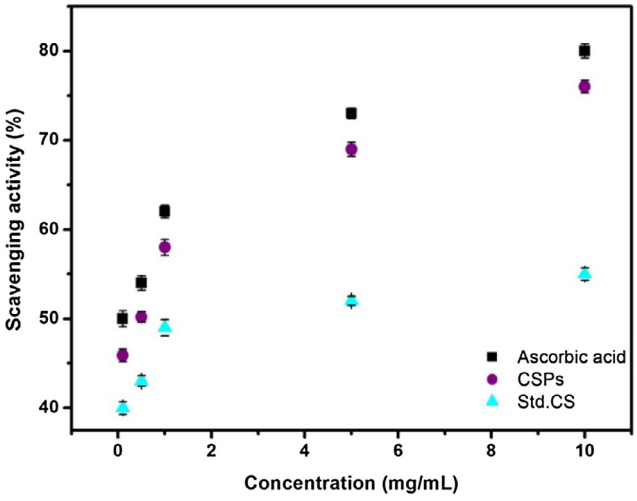

Fig. 7 Scavenging ability of ascorbic acid, CSPs, and Std.CS on 1, 1-diphenyl-2-picrylhydrazyl radicals.

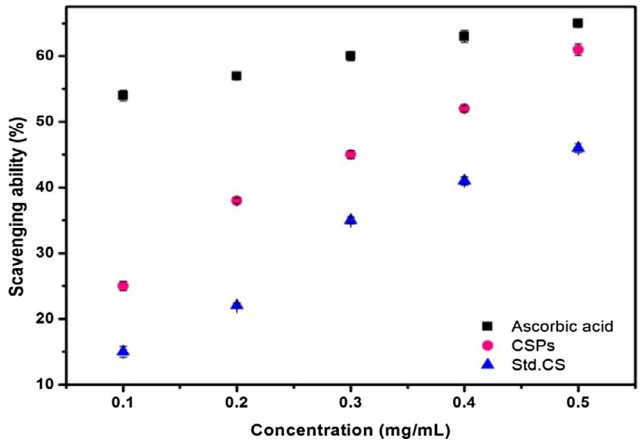

Fig. 6 Superoxide radical scavenging ability of ascorbic acid, CSPs, and Std. CS.

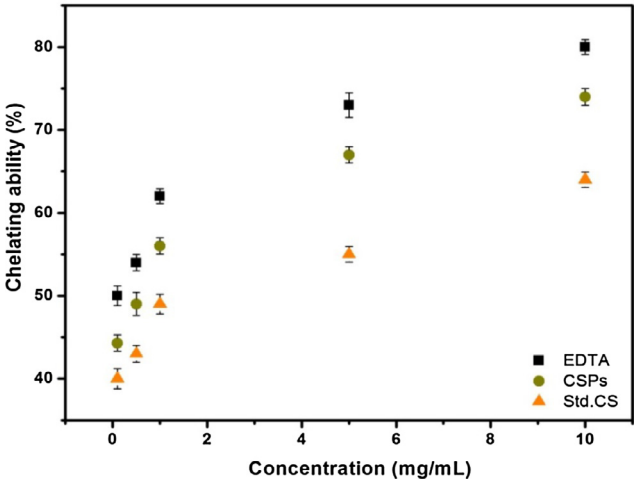

Fig. 8 Chelating ability of EDTA, CSPs, and Std. CS on ferrous ions.

Therefore, we anticipate that CSPs have the potential to become a powerful and safe natural antimicrobial agent. Moreover, their antioxidant properties, including reducing power, scavenging and chelating ability, suggest that the submicron particles synthesized using our mechanochemical technique can enhance antioxidant activity in a biological system. Overall, the gladius, typically discarded as waste, can be used in the mechanochemical production of CSPs for biomedical applications.

Conflict of Interest

The authors declare no conflict of interest.

Compliance with Ethics Requirement

The article does not contain any studies with human or animal subjects.

Acknowledgments

The authors thank Dongguk University, Seoul, Republic of Korea, for providing research facilities. The encouragement and support rendered by the Management of Loyola College, Chennai, India, is gratefully acknowledged. The authors also extend their sincere appreciation to the Deanship of Scientific Research at King Saud University for its funding to this Prolific Research Group (PRG-1437-28).

References

[1] Abdou ES, Nagy KSA, Elsabee MZ. Extraction and characterization of chitin and chitosan from local sources. Bioresour Technol 2008;99:1359–67.
[2] Kaya M, Baran T, Mentes A, Asaroglu M, Sezen G, Tozak KO. Extraction and characterization of α-chitin and chitosan from six different aquatic invertebrates. Food Biophys 2014;9:145–57.
[3] Tasar OC, Erdal S, Taskin M. Chitosan production by psychrotolerant *Rhizopusoryzae* in non-sterile open fermentation conditions. Int J Biol Macromol 2016;89:428–33.
[4] Jung J, Zhao Y. Characteristics of deacetylation and depolymerisation of β-chitin from jumbo squid (*Dosidicusgigas*) pens. Carbohydr Res 2011;346:1876–84.
[5] Reys LL, Silva SS, Oliveria JM, Caridade SG, Mano JF, Silva TH, et al. Revealing the potential of squid chitosan-based structures for biomedical applications. Biomaterials 2013;8(4): 045002.
[6] Youn DK, No HK, Prinyawiwatkul W. Preparation and characterisation of selected physicochemical and functional properties of β-chitosan from squid pen. Int J Food Sci Technol 2013;48(8):1661–9.
[7] Arbia W, Arbia L, Adour L, Amrane A. Chitin extraction from crustacean shells using biological methods. Food Technol Biotechnol 2013;51(1):12–25.
[8] Ding F, Deng H, Du Y, Shi X, Wang Q. Emerging chitin and chitosan nanofibrous materials for biomedical applications. Nanoscale 2014;6:9477–93.
[9] Nahaei M, Valizadeh H, Baradaran B, Nahaei MR, Asgari D, Nezhadi H, et al. Preparation and characterization of chitosan/β-cyclodextrin submicron particles containing plamid DNA encoding interleukin-12. Drug Res 2012;63:7–12.
[10] Victor TT, Atanasova G, Aquil A, Filee P, Garbacki N, Vanhooteghem O, et al. Development of a chitosan nanofibrillar scaffold for skin repair and regeneration. Biomacromol 2011;12 (9):3194–204.
[11] Kong M, Chen XG, Xing K, Park HJ. Antimicrobial properties of chitosan and mode of action: a state of the art review. Int J Food Microbiol 2010;144:51–63.
[12] Charernsriwilaiwat N, Opanasopit P, Rojanarata T, Ngawhirunat T. *In vitro* antioxidant activity of chitosan aqueous solution: effect of salt form. Trop J Pharm Res 2012;11(2):235–42.
[13] Guo Y, Chu M, Tan S, Zhao S, Liu H, Otieno BO, et al. Chitosan-g-TPGS submicron particles for anticancer drug delivery and overcoming multidrug resistance. Mol Pharm 2014;11(1):59–70.
[14] Friedman AJ, Phan J, Schairer DO, Champer J, Qin M, Pirouz A, et al. Antimicrobial and anti-inflammatory activity of chitosan- alginate submicron particles: a targeted therapy for cutaneous pathogens. J Invest Dermatol 2012;133:1231–9.
[15] Ma JX, Li Q, Zhou Y. Stimulation effect of chitosan on the immunity of radiotherapy patients suffered from lung cancer. Int J Biol Macromol 2015;72:195–8.
[16] Santhosh S, Sini R, Anandan R, Mathew PT. Hepatoprotective activity of chitosan against isoniazid and rifampicin- induced toxicity in experimental rats. Eur J Pharmacol 2007;572:69–73.
[17] Zhang W, Zhang J, Jiang QX, Xia W. Physicochemical and structural characteristics of chitosan nanopowders prepared by ultrafine milling. Carbohydr Polym 2012;87(1):309–13.
[18] Yang HC, Wang WH, Huang KS, Hon MH. Preparation and application of nanochitosan to finishing treatment with anti-microbial and anti-shrinking properties. Carbohydr Polym 2010;79(1):176–9.
[19] Focher B, Beltrame PL, Naggi A, Torri G. Alkaline N-Deacetylation of chitin enhanced by flash treatments-reaction kinetics and structure modifications. Carbohydr polym 1990;12 (4):405–18.
[20] Baxter A, Dillion M, Taylor KDA, Roberts GAF. Improved method for i.r. determination of the degree of N- acetylation of chitosan. Int J Biol Macromol 1992;14(3):166–9.
[21] Bronswijk WV. Molecular weight determination by viscometry. In: Handbook of physical chemistry 301/302 for student in department ofchemistry. Australia: Western Australian Institute of Technology; 1975. p. 127–30.
[22] AOAC. Official methods of analysis of the Association of Official Analytical Chemistry. 14th ed. Washington, DC: The Association of Official Analytical Chemistry, Inc.; 1984.
[23] Wang JC, Kinsella JE. Functional properties of novelproteins: alfalfa leaf protein. J Food Sci 1976;41:286–92.
[24] Balachandran C, Duraipandiyan V, Emi N, Ignacimuthu S. Antimicrobial and cytotoxic properties of Streptomyces sp. (ERINLG-51) isolated from Southern Western Ghats. South Ind J Biol Sci 2015;1(1):7–14.
[25] Yen MT, Yang JH, Mau JL. Antioxidant properties of chitosan from crab shells. Carbohydr Polym 2008;74:840–4.
[26] Jing TY, Zhao XY. The improved pyrogallol method by using terminating agent for superoxide dismutase measurement. Prog Inorg Biochem Biophys 1995;22:84–6.
[27] Ramasamy P, Subhapradha N, Shanmugam V, Shanmugam A. Extraction, characterization and antioxidant property of chitosan from cuttlebone *Sepia kobiensis* (Hoyle 1885). Int J Biol Macromol 2014;64:202–12.
[28] Lavall RL, Assi OB, Campana-Filho SP. Beta chitin from the pens of Loligo sp.: extraction and characterization. Bioresour Technol 2007;98(13):2465–72.
[29] Zouhour L, Salah S, Saloua S, Amor EA. Extraction and characterization of chitin and chitosan from crustacean by-products- biological and physicochemical properties. Afr J Biotechnol 2010;10(4):640–7.

[30] Kurita K, Tomita K, Tada T, Ishii S, Nishimura SI, Shimoda K. Squid chitin as a potential alternative chitin source: deacetylation behavior and characteristic properties. J Polym Sci A Polym Chem 1993;31:485–91.
[31] Muzzarelli C, Francescangeli O, Tosi G, Muzzarelli RAA. Susceptibility of dibutyryl chitin and regenerated chitin fibres to deacylation and depolymerization by lipases. Carbohydr polym 2004;56(2):137–46.
[32] Huang J, Zhao D, Hu S, Wei J, Mei L. Biochemical activities of low molecular weight chitosan derived from squid pen. Carbohydr polym 2012;87:2231–6.
[33] Gómez-Estaca J, López de Lacey A, López-Caballero ME, Gómez-Guillén MC, Montero MP. Biodegradable gelatin chitosan films incorporated with essential oils as antimicrobial agents for fish preservation. Food Microbiol 2010;27(7):889–96.
[34] Yen MT, Tseng YH, Li RC, Mau JL. Antioxidant properties of fungal chitosan from shiitake stipes. LWT – Food Sci Technol 2007;40:255–61.
[35] Prabu K, Natarajan E. *In vitro* antimicrobial and antioxidant activity of chitosan isolated from *Podophthalmus vigil*. J Appl Pharm Sci 2012;2:75–82.
[36] Yasufuku T, Anraku M, Kondo Y, Hata T, Hirose J, Kobayashi N, et al. Useful extend-release chitosan tablets with high antioxidant activity. Pharmaceutics 2010;2:245–57.
[37] Huang M, Fong CW, Khor E, Lim LY. Transfection efficiency of chitosan vectors: effect of polymer molecular weight and degree of deacetylation. J Control Release 2005;106:391–406.
[38] Qin Y. The chelating properties of chitosan fibers. J Appl Polym Sci 1993;49:727–31.